Accepted Manuscript

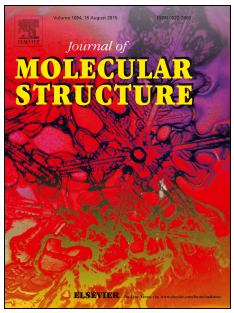

Synthesis and characterization of sterically and electrostatically shielded pyrrolidine nitroxide radicals

Lisa Lampp, Uwe Morgenstern, Kurt Merzweiler, Peter Imming, Rüdiger W. Seidel

PII: S0022-2860(19)30021-3

DOI: https://doi.org/10.1016/j.molstruc.2019.01.015

Reference: MOLSTR 26066

To appear in: *Journal of Molecular Structure*

Received Date: 15 November 2018

Revised Date: 3 January 2019

Accepted Date: 4 January 2019

Please cite this article as: L. Lampp, U. Morgenstern, K. Merzweiler, P. Imming, Rü.W. Seidel, Synthesis and characterization of sterically and electrostatically shielded pyrrolidine nitroxide radicals, *Journal of Molecular Structure* (2019), doi: https://doi.org/10.1016/j.molstruc.2019.01.015.

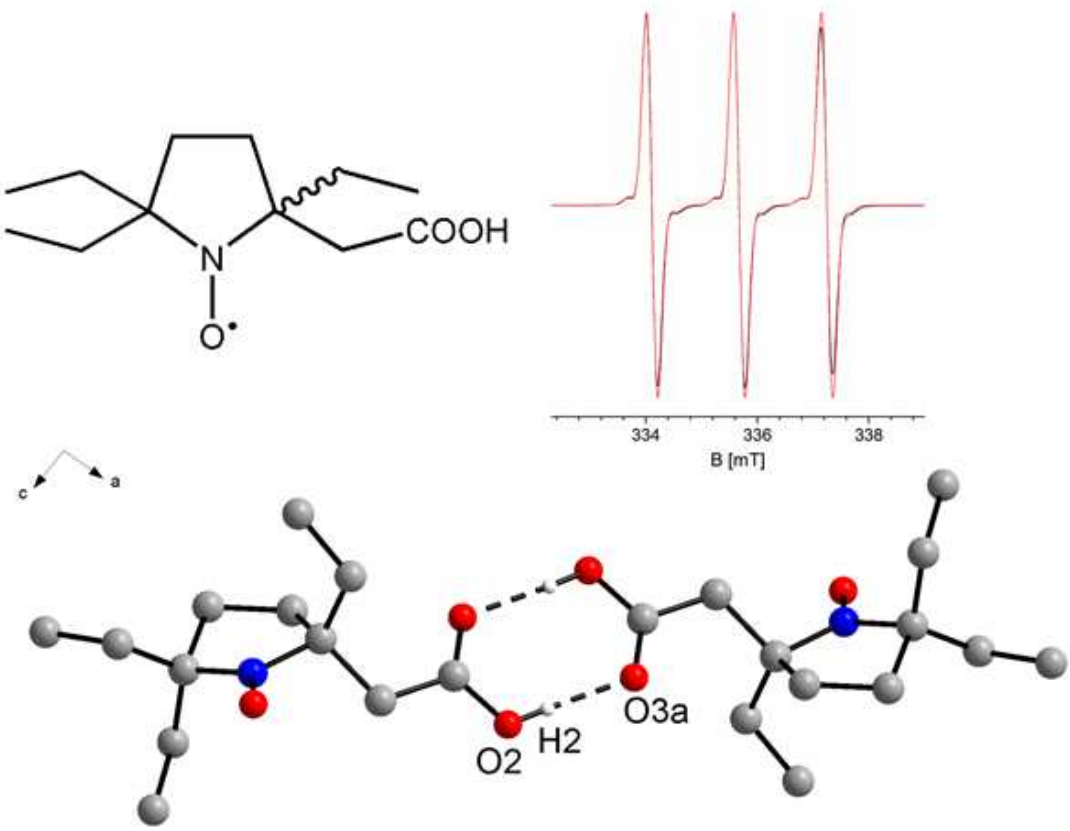

Synthesis and characterization of sterically and electrostatically shielded pyrrolidine nitroxide radicals[#]

Lisa Lampp[a], Uwe Morgenstern[b], Kurt Merzweiler[b], Peter Imming*[a], Rüdiger W. Seidel*[a]

[a] Institut für Pharmazie, Martin-Luther-Universität Halle-Wittenberg, Wolfgang-Langenbeck-Str. 4, 06120 Halle (Saale), Germany

[b] Institut für Chemie, Martin-Luther-Universität Halle-Wittenberg, Kurt-Mothes-Straße 2, 06120 Halle (Saale), Germany

---

[#]Dedicated to Professor Martin Feigel on the occasion of his 70th birthday.

*Corresponding authors

E-Mail: peter.imming@pharmazie.uni-halle.de, ruediger.seidel@pharmazie.uni-halle.de

Abstract

Two new pyrrolidine nitroxide radicals, *cis*/*trans*-2,5-bis(carboxymethyl)-2,5-diethylpyrrolidine 1-oxyl and 2-(carboxymethyl)-2,5,5-triethylpyrrolidine 1-oxyl, for potential applications as spin probes and labels are reported. Carboxymethyl and ethyl groups have been introduced in the α-positions of the nitroxide group in order to improve the stability of the radicals through steric and electrostatic shielding. The compounds were structurally characterized by X-ray crystallography and EPR spectroscopy. An ascorbic acid reduction assay proves that the newly synthesized radicals exhibit higher reductive stability than the well-known and commercially available nitroxide radicals 3-carboxy-PROXYL and 4-carboxy-TEMPO.

Keywords: spin label; nitroxide; radical; crystal structure, EPR spectroscopy

Introduction

Electron paramagnetic resonance (EPR) spectroscopy is a useful analytical method for the elucidation of the structure and dynamic behavior of paramagnetic compounds and their microenvironment [1]. Most polymeric materials and biomolecules are diamagnetic and thus EPR silent. The absence of an EPR signal in most (bio)materials provides analytical and diagnostic possibilities through artificial introduction of a paramagnetic centre *via* spin probing and labelling [2-4].

Radicals based on the nitroxide group (N–O$^{\bullet}$) are by far still the most widely used compounds for spin probing and labeling [5]. Typical nitroxide radicals are based on piperidine, pyrrolidine or other nitrogen heterocycles. In these compounds, the nitroxide moiety, where the unpaired electron is mainly located, is flanked by two quaternary carbon atoms, which provide steric shielding. The absence of α-hydrogen atoms prevents nitrone formation. 3-Carboxy-PROXYL (**3-CP**) and 4-carboxy-TEMPO (**4-CT**) are two well-known and commercially available nitroxide radicals (Scheme 1). *In vivo*, common nitroxide radicals are, however, reduced within minutes, which limits biological applications. Thus, attempts have been made to increase the reductive stability [6, 7].

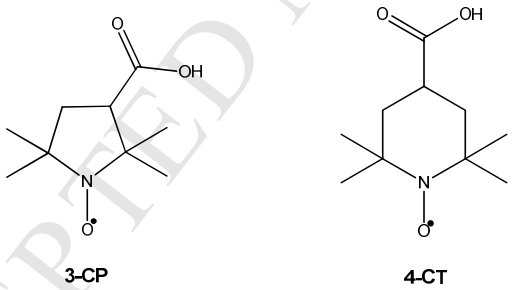

Scheme 1 Chemical diagrams of 3-carboxy-PROXYL (**3-CP**) and 4-carboxy-TEMPO (**4-CT**).

We have synthesized and studied two new pyrrolidine nitroxide radicals for spin labelling and potential *in vivo* use as spin probes. Carboxymethyl and ethyl groups were tethered to the α-positions of the nitroxide group to achieve higher reductive stability. Electrostatic shielding through ionizable groups, such as carboxymethyl, could increase the stability of the radicals further [7, 8]. We report the synthesis and structural elucidation of 2,5-bis(carboxymethyl)-2,5-diethylpyrrolidine 1-oxyl and 2-(carboxymethyl)-2,5,5-triethylpyrrolidine 1-oxyl. The reductive stability of the new radicals was assessed through an ascorbic acid reduction assay.

Experimental section

General

Starting materials were obtained from commercial sources and used as received. The nitroxide radicals **3-CP** and **4-CT** were purchased from Sigma-Aldrich. Solvents were of reagent grade. Diethyl ether used for Grignard reactions was dried over sodium metal and freshly distilled before use. Methanol used for the preparation of a sodium methoxide solution was dried over molecular sieve. Grignard reactions and reactions with sodium metal were carried out under argon using standard Schlenk techniques. 6-Nitrooctane-3-one (**1**) was prepared from 1-nitropropane and ethyl vinyl ketone following the method described by McMurry and Melton [9]. The spectral properties agreed with those reported in the literature [10]. 3-Nitropentane was synthesized from pentane-3-amine using *meta*-chloroperoxybenzoic acid as oxidizing agent, as described by Gilbert and Borden [11]. The spectral properties were in accord with those published previously [12]. Column chromatography was performed on silica gel 60 (70-230 mesh or 230-400 mesh). The purity of all compounds and the progress of the reactions were monitored by thin layer chromatography using silica gel 60 F254 plates (Merck KGaA, Darmstadt, Germany). Visualizations were accomplished with an UV lamp (254 nm) or iodine staining. The R_f values given are uncorrected. ^{1}H and ^{13}C NMR spectra were recorded on an Agilent Technologies VNMRS 400 MHz or a Varian Inova 500 MHz spectrometer. Chemical shifts (δ) are reported relative to the residual solvent peak of $CDCl_3$ as internal standard: δ_H = 7.26 ppm, δ_C = 77.0 ppm. Infrared (IR) spectra were recorded on a Bruker IFS 28 FTIR spectrometer equipped with a Thermo Spectra-Tech attenuated total reflection (ATR) unit with a 20 mm ZnSe-Fresnel crystal. High resolution mass spectra (HRMS) were measured on a LTQ-Orbitrap-XL (ESI source) of Thermo Scientific. Samples were dissolved in chloroform / methanol.

Synthesis

2,5-Diethyl-3,4-dihydro-2*H*-pyrrole 1-oxide (2): Zinc powder (33.0 g, 505 mmol) was added in small portions to a stirred solution of 6-nitrooctane-3-one (22.0 g, 127 mmol) and ammonium chloride (7.4 g, 138 mmol) in 170 mL of water cooled with an ice bath, ensuring that the temperature of the reaction mixture did not exceed 10 °C. Subsequently, the mixture was continued to stir for 12 h while allowing to warm up to room temperature. The reaction

mixture was filtered through celite and the residue was rinsed with a small amount of methanol. The filtrate was concentrated in vacuum and extracted seven times with 20 mL of chloroform. The combined organic layers were dried over magnesium sulfate and the solvent was removed was removed under reduced pressure. The crude product was purified by distillation under reduced pressure (0.17 mbar, b.p. 94-96 °C). Yield: 14.60 g (103 mmol, 72 %). ^{1}H NMR(400 MHz, $CDCl_3$): δ 3.94 (m, *J* = 10.4, 5.1, 3.4, 1.8 Hz, NCH, 1H), 2.60 (m, *J* = 7.6, 3.3, 1.7 Hz, CH_2, 2H), 2.51 (m, *J* = 12.5, 7.8, 6.2, 3.2, 1.5 Hz, CH_2, 2H), 2.28 – 2.15 (m, CH_2, 1H), 2.09 (m, *J* = 13.7, 7.6, 3.4 Hz, CH_2, 1H), 1.82 – 1.61 (m, CH_2, 2H), 1.09 (t, *J* = 7.7 Hz, CH_3, 3H), 0.90 (t, *J* = 7.5 Hz, CH_3, 3H). ^{13}C NMR(101 MHz, $CDCl_3$): δ 147.87, 73.50, 28.75, 25.16, 22.00, 19.95, 9.35, 8.79. HRMS(ESI): calcd. for $C_8H_{16}NO$ $[M+H]^+$ 142.1232, found 142.1221.

2-Allyl-2,5-diethyl-3,4-dihydro-2*H*-pyrrole 1-oxide (3): compound **2** (3.0 g, 21.24 mmol) dissolved in 7 mL of diethyl ether was added dropwise to a stirred solution (31.9 mL) of allylmagnesium bromide (1.0 M) in diethyl ether at −10 °C. After stirring for 12 h while allowing the mixture to warm up to room temperature, 2.5 ml of a saturated aqueous solution of ammonium chloride and 2.5 mL of water were successively added. After filtration through a frit, the diethyl ether phase was separated, washed with brine and evaporated. The residue was taken up with 43 mL of methanol containing 1.1 mL of conc. ammonia and anhydrous copper(II) acetate (0.12 g, 0.045 mmol). Oxygen was bubbled through the mixture with stirring until the color turned dark blue. Afterwards, the solvent was removed under reduced pressure and the residue was taken up with 20 mL of chloroform. After washing successively with a saturated solution of sodium bicarbonate (3 × 20 mL) and brine (20 mL) and drying over magnesium sulfate, the solvent was removed under reduced pressure. The crude product was purified by column chromatography (ethyl acetate/methanol 9:1, R_f = 0.19). Yield: 2.43 g (13.41 mmol, 60 %). ^{1}H NMR (400 MHz, $CDCl_3$) δ 5.66 (m, *J* = 17.1, 10.1, 8.5, 6.1 Hz, CH_2=$\underline{CH}CH_2$, 1H), 5.18 – 5.06 (m, $\underline{CH_2}$=$CHCH_2$, 2H), 2.72 – 2.60 (m, CH_2=$CH\underline{CH_2}$, 1H), 2.50 (m, *J* = 7.9 Hz, $\underline{CH_2}CH_3$, 4H), 2.25 (m, *J* = 13.8, 8.6, 0.8 Hz, CH_2=$CH\underline{CH_2}$, 1H), 2.10 – 1.50 (m, CH_2CH_2, 4H), 1.09 (t, *J* = 7.6 Hz, CH_3, 3H), 0.84 (t, *J* = 7.4 Hz, CH_3, 3H). ^{13}C NMR (101 MHz, $CDCl_3$) δ 147.42, 132.73 , 119.16 , 79.31 , 41.85 , 30.28 , 27.78 , 24.32 , 19.99 , 9.49 , 7.66. HRMS(ESI): calcd. for $C_{11}H_{20}NO$ $[M+H]^+$ 182.1545, found 182.1533.

2,5-Diallyl-2,5-diethylpyrrolidine 1-oxyl (4): compound **3** (0.98 g, 5.41 mmol) dissolved in 2 mL of diethyl ether was added dropwise to a stirred solution (8.1 mL) of allylmagnesium bromide (1.0 M) in diethyl ether at −10 °C. After stirring for 1.5 h, a saturated solution of ammonium chloride (1 mL) and water were (1 mL) were successively added. The mixture

was filtered through a frit, and the residue was rinsed successively with small amounts of saturated ammonium chloride solution and diethyl ether. The diethyl ether phase was separated and washed with brine. The aqueous phase was extracted once with diethyl ether and the organic layers were combined and the solvent was removed under reduced pressure. The residue was taken up with 11 mL of methanol containing 0.3 mL of conc. ammonia and anhydrous copper(II) acetate (26 mg, 0.146 mmol). Oxygen was bubbled through the mixture with stirring, which was stopped 30 min after the color of the mixture had turned dark blue. Subsequently, the solvent was removed under reduced pressure. The crude product was purified by column chromatography (ethyl acetate/*n*-heptane 1:9, R_f = 0.38), to give **5** as orange liquid. Yield: 0.85 g (3.84 mmol, 71 %). HRMS (ESI): calcd. for $C_{14}H_{24}NO$ $[M]^+$ 222.1851, found 222.1851. IR(ATR): 3076, 3005, 2965, 2938, 2880, 1639, 1462, 1441, 1434, 1407, 1380, 1312, 1292, 1218, 996, 965, 912, 797 cm^{-1}.

2,5-Bis(carboxymethyl)-2,5-diethylpyrrolidine 1-oxyl (5): compound **4** (0.7 g, 3.15 mmol) was added to a suspension of potassium permanganate (2.96 g, 18.89) and 18-crown-6 (0.33 g, 1.26 mmol) in 25 mL of benzene and stirred for 48 h at room temperature. Subsequently, the mixture was filtered and successively with a 5 % aqueous sodium hydroxide solution and water. The combined aqueous layers were acidified with hydrochloric acid and extracted several times with chloroform. The combined organic layers were dried over magnesium sulfate and the solvents were removed under reduced pressure. The crude product was purified and the *cis*- and *trans*-diastereomers partly separated by repeated column chromatography [chloroform/methyl *tert*-butyl ether/acetic acid 4:6:0.2, R_f(*cis*) = 0.40, R_f(*trans*) = 0.55]. Yield: 0.10 g (0.39 mmol, 12 %, *cis*/*trans* 1:1). IR(ATR): 3682-2222, 3018, 2979, 2969, 2935, 2884, 2745, 2666, 2634, 2570, 1694, 1460, 1447, 1408, 1346, 1329, 1312, 1274, 1255, 1232, 1203, 1156, 1123, 1092, 1068, 1015, 990, 977, 941, 916, 889, 916, 799, 714 cm^{-1}. Crystals of ***cis*-5** suitable for single-crystal X-ray analysis were grown from a solution in chloroform/toluene (1:1) by the slow-evaporation method. ***trans*-5**: HRMS(ESI): calcd. for $C_{12}H_{21}NO_5$ $[M+H]^+$ 259.1420, found 259.1410. IR (ATR): 3585-2295, 2970, 2942, 2883, 1776, 1704, 1463, 1412, 1385, 1309, 1188, 1177, 1120, 955, 931, 905, 878, 846, 825, 801, 736 cm^{-1}.

6-Ethyl-6-nitrooctan-3-one (6): To prepare a solution of sodium methoxide, sodium metal (0.49 g, 21.26 mmol) was placed in a flask and 15 mL of methanol were added dropwise, so that the solution boiled gently. Subsequently, 3-nitropentane (3.0 g, 25.61 mmol) was added with stirring. To the stirred solution, ethyl vinyl ketone (1.88 g, 22.35 mmol) was added dropwise. After stirring for 4.5 h, 2 mL of glacial acetic acid were added dropwise and the

solvent was removed under reduced pressure. The residue was partioned between water and dichloromethane. The organic layer was separated and washed successively with 10 % aqueous solution of sodium carbonate and brine. After drying over magnesium sulfate, the solvent was removed under reduced pressure. The compound was purified by distillation under reduced pressure (0.14 mbar, b.p. 110-113 °C) to give a pale yellow liquid. Yield: 2.37 g (11.78 mmol, 53 %). ^{1}H NMR(500 MHz, $CDCl_3$): δ 2.47-2.39 (q, CH_2, 2H), 2.38 – 2.14 (m, CH_2, 4H), 2.06-1.83 (m, CH_2, 4H), 1.06 (t, *J* = 7.4, 1.0 Hz, CH_3, 3H), 0.86 (t, *J* = 7.5, 1.0 Hz, CH_3, 6H). ^{13}C NMR(101 MHz, $CDCl_3$): δ 209.27, 94.65, 36.32, 36.04, 28.80, 27.70, 8.05, 7.75. HRMS(ESI): calcd. for $C_{10}H_{20}NO_3$ $[M+H]^+$ 202.1443, found 202.1438.

2,2,5-Triethyl-3,4-dihydro-2*H*-pyrrole 1-oxide (7): compound **6** (1.80 g, 8.94 mmol) was added to a solution ammonium chloride (0.52 g, 9.66 mmol) in 12 mL of water. The mixture was cooled to ca. −10 °C and zinc powder (2.34 g, 35.8 mmol) was added in small portions, ensuring that the temperature of the reaction mixture did not exceed 10 °C. Afterwards, the mixture was filtered through Celite®545 and the residue was rinsed with a small amount of methanol. The filtrate was concentrated in vacuum and extracted with chloroform (5 × 10 mL). The combined organic layers were dried over magnesium sulfate and, subsequently, the solvent was reduced under reduced pressure. The crude product was purified by column chromatography (chloroform/methanol 10:0.2, R_f = 0.13) to give **7** as an orange liquid. Yield: 1.49 g (8.80 mmol, 98 %). ^{1}H NMR (400 MHz, $CDCl_3$): δ 2.59-2.44 (m, CH_2CH_2, 4H), 2.00-1.49 (m, $CH_3\underline{CH_2}$, 6H), 1.09 (t, *J* = 7.7, 1.4 Hz, 3H), 0.81 (t, *J* = 7.4, 1.6 Hz, 6H) ppm. ^{13}C NMR (101 MHz, $CDCl_3$): δ 147.47, 80.00, 77.32, 77.21, 77.01, 76.69, 30.31, 27.86, 24.19, 19.97, 9.45, 7.67 ppm. HRMS(ESI): calcd. for $C_{10}H_{20}NO$ $[M+H]^+$ 170.1545, found 170.1535.

2-Allyl-2,5,5-triethylpyrrolidine 1-oxyl (8): compound **7** (1.00 g, 5.91 mmol) dissolved in 2 mL of diethyl ether was added dropwise to a solution (8.9 mL) of allylmagnesium bromide (1.0 M) in diethyl ether with stirring at −10 °C. After stirring for 1.5 h, successively 1 mL of a saturated aqueous solution of ammonium chloride and 1 mL of water were added dropwise. Subsequently, the reaction mixture was filtered through a frit and the residue was rinsed successively with small amounts of diethyl ether and a saturated aqueous solution of ammonium chloride. The diethyl ether phase was separated and washed with brine. After evaporation of the solvent, the residue was taken up with 11 mL of methanol containing 0.3 mL of conc. ammonia and anhydrous copper(II) acetate (0.03 g, 0.16 mmol). Oxygen was bubbled through the mixture with stirring, which was stopped 30 min after the color of the mixture had turned dark blue. Subsequently, the solvent was removed under reduced pressure. The crude product was purified by column chromatography (ethyl acetate/*n*-heptane 1:9, R_f =

0.48) to give **7** as an orange liquid. Yield: 0.83 g (3.95 mmol, 67 %). HRMS(ESI): calcd. for $C_{13}H_{24}NO$ $[M]^+$ 210.1858, found 210.1848. IR(ATR): 3076, 2965, 2937, 2879, 1639, 1462, 1444, 1406, 1380, 1347, 1331, 1314, 1295, 1219, 1554, 1112, 997, 968, 953, 913, 888, 866, 849, 800, 734 cm^{-1}.

2-(Carboxymethyl)-2,5,5-triethylpyrrolidine 1-oxyl (9): compound **8** (0.6 g, 2.85 mmol) was added to a suspension of potassium permanganate (2.71 g, 17.12 mmol) and 18-crown-6 (0.30 g, 1.14 mmol) in 23 mL of benzene and stirred for 24 h at room temperature. Subsequently, the mixture was filtered and successively with a 5 % aqueous sodium hydroxide solution and water. The combined aqueous layers were acidified with hydrochloric acid and extracted once with chloroform. The combined organic layers were dried over magnesium sulfate and the solvents were removed under reduced pressure. The crude product was purified by column chromatography (chloroform/acetic acid 10:0.2, R_f = 0.50) to give **9** as a pale yellow solid. Yield: 0.19 g (0.83 mmol, 29 %). HRMS (ESI): calcd. for $C_{12}H_{22}NO_3$: $[M]^+$ 228.1600, found 228.1600. IR(ATR): 3408-2242, 3089, 3024, 2965, 2939, 2924, 2881, 2740, 2658, 2633, 2546, 1703, 1459, 1455, 1426, 1407, 1376, 1339, 1328, 1290, 1260, 1234, 1218, 209, 1160, 1140, 975, 961, 926, 890, 880 cm^{-1}.

Single-crystal X-ray analysis

The X-ray intensity data were collected on a STOE IPDS 2T diffractometer for ***cis*-5** and on a STOE IPDS II for **9**, using graphite-monochromated Mo-K_α radiation. The crystal structures were solved with SHELXT [13] and refined with SHELXL-2018/3 [14]. The OLEX2 software was used as a graphical interface [15]. Anisotropic atomic displacement parameters were introduced for all non-hydrogen atoms. With the exception of the methyl and carboxy groups in ***cis*-5**, hydrogen atoms were placed at geometrically calculated positions and refined with the appropriate riding model, with U_{iso}(H) = 1.2 U_{eq}(C, O) (1.5 for methyl groups). The O–H distances in ***cis*-5** were restrained to a target value of 0.84(2) Å and with U_{iso}(H) = 1.2 U_{eq}(O). Due to the rather low quality of the crystals of **9**, the *R*1 and *wR*2 values are higher than in the case of ***cis*-5**. Representations of the crystal and molecular structures were drawn with DIAMOND [16]. Crystal data and refinement details for ***cis*-5** and **9** are listed in Table 1.

CCDC 1876526 (***cis*-5**) and 1876527 (**9**) contains the supplementary data for this paper. These data can be obtained free of charge from The Cambridge Crystallographic Data Centre *via* http://www.ccdc.cam.ac.uk/structures.

EPR measurements

1 mM solutions of ***cis*-5**, ***trans*-5**, **9** and **3-CP** in 2.3 M actetate buffer pH 4.5 (Ph. Eur.), 0.08 M phosphate buffer pH 7.4 (Ph. Eur.) and 1.5 M tris-HCl buffer pH 8.8 (Ph. Eur.) were prepared. EPR spectra were measured in 50 µl capillaries using an X-band EPR spectrometer at 9.30 – 9.55 GHz (Miniscope MS 400, Magnettech, Berlin, Germany) at 25 °C under atmospheric oxygen. General settings were as follows: microwave power, 3.162 mW; sweep, 11.715 mT; scan time, 60 s; modulation frequency, 100 kHz; modulation amplitude, 100 µT. EPR spectra were analyzed using the MATLAB toolbox EasySpin. Determination of the hyperfine coupling constants a and peak-to-peak linewidths (ΔB_{pp}) was carried out by simulation of each spectrum, using EasySpin‘s function *garlic*.

Ascorbic acid reduction assay

100 µl radical solution (***cis*-5, *trans*-5**, **9**, **3-CP**, **4-CT**, c = 1 mM) in phosphate buffer pH 7.4 (50 mM, 2 mM EDTA) were mixed with 100 µl ascorbic acid solution (c = 10 mM in phosphate buffer pH 7.4, 50 mM with 2 mM EDTA). After mixing EPR spectra were measured every 2 minutes in 50 µl capillaries using an X-band EPR spectrometer at 9.30 – 9.55 GHz (Miniscope MS 400, Magnettech, Berlin, Germany) at 25 °C under atmospheric oxygen. General settings were as follows: microwave power, 3.162 mW; sweep, 11.715 mT; scan time, 60 s; modulation frequency, 100 kHz; modulation amplitude, 30 µT. Second-order rate constants k ($M^{-1}s^{-1}$) for the initial rates of reduction were obtained from the decay of the low-field EPR peak height by using a literature protocol [17].

Table 1 Crystal data and refinement details for **cis-5** and **9**.

	***cis*-5**	**9**
Empirical formula	$C_{12}H_{20}NO_5$	$C_{12}H_{22}NO_3$
*M*r	258.29	228.30
λ (Å)	0.71073	0.71073
Crystal size (mm)	$0.50 \times 0.18 \times 0.15$	$0.246 \times 0.221 \times 0.164$
Crystal system	Monoclinic	Monoclinic
Space group	$P2_1/n$	$P2_1/n$
T (K)	200(2)	213(2)
a (Å)	8.4588(8)	8.9620(7)
b (Å)	9.5452(6)	9.5965(5)
c (Å)	16.2549(14)	15.0929(12)
β (°)	97.014(7)	93.166(6)
V (Å^3)	1302.61(19)	1296.07(16)
Z	4	4
ρ_{calc} (g cm^{-3})	1.317	1.170
μ (mm^{-1})	0.102	0.083
F(000)	556	500
θ range (°)	4.243-29.278	2.516-25.000
Reflections collected / unique	14319 / 3503	8125 / 2288
R_{int}	0.0386	0.0420
Observed reflections [$I > 2\sigma(I)$]	2166	1691
Goodness-of-fit on F^2	0.858	1.036
Parameters / restraints	171 / 2	145 / 0
*R*1 [$I > 2\sigma(I)$]	0.0390	0.0697
*wR*2 (all data)	0.0940	0.2226
Residuals (eÅ^{-3})	0.239 / –0.153	0.698 / –0.286

Results and discussion

Synthesis

The synthetic route to pyrrolidine nitroxide radicals (Scheme 2) was adapted from Hideg and Lex [18, 19]. The γ-nitroketones **1** and **6** were prepared by Michael addition of the respective nitroalkane to an α,β-unsaturated ketone in the presence of a base [9, 10]. **1** and **6** were reduced to the corresponding hydroxylaminoketones, which cyclized *in situ* to yield the nitrones **2** and **7**, using zinc powder and ammonium chloride [20]. The nitrones **2** and **7** were treated with the Grignard reagent allyl magnesium bromide to give the corresponding *N*-hydroxy derivatives, which were not isolated but directly oxidized to obtain the *N*-oxyl radicals **4** and **8**, using Cu^{II} as catalyst. The latter two steps had to be carried out twice to obtain **4** *via* **3**. Successful quantitative oxidation of the *N*-hydroxy intermediates to the *N*-oxyl radicals **4** and **8** was confirmed by the absence of O–H stretching bands in the IR spectra, which would appear in range 3500-3600 cm^{-1} (*e. g.* 3580 cm^{-1} was reported for 2,2,6,6-tetramethylpiperidine *N*-hydroxylamine [21]). The IR bands observed at 3076 cm^{-1} for both **4** and **8** are characteristic of the C–H stretching vibrations of the terminal alkenyl groups. Compounds **4** and **8** were converted to the carboxymethyl derivatives **5** and **9**, respectively, by oxidative cleavage of the terminal double bonds with potassium permanganate. The broad bands in the range of 3500-2500 cm^{-1} in the IR spectra of **5** and **9** are typical of carboxy O–H stretching vibrations. The *cis*- and *trans*- diastereomers of **5** were separated by column chromatography. The positions of the carbonyl stretching bands for ***cis*-5** (1694 cm^{-1}) and ***trans*-5** (1705 cm^{-1}) differ in the IR spectra within spectral resolution (4 cm^{-1}),.

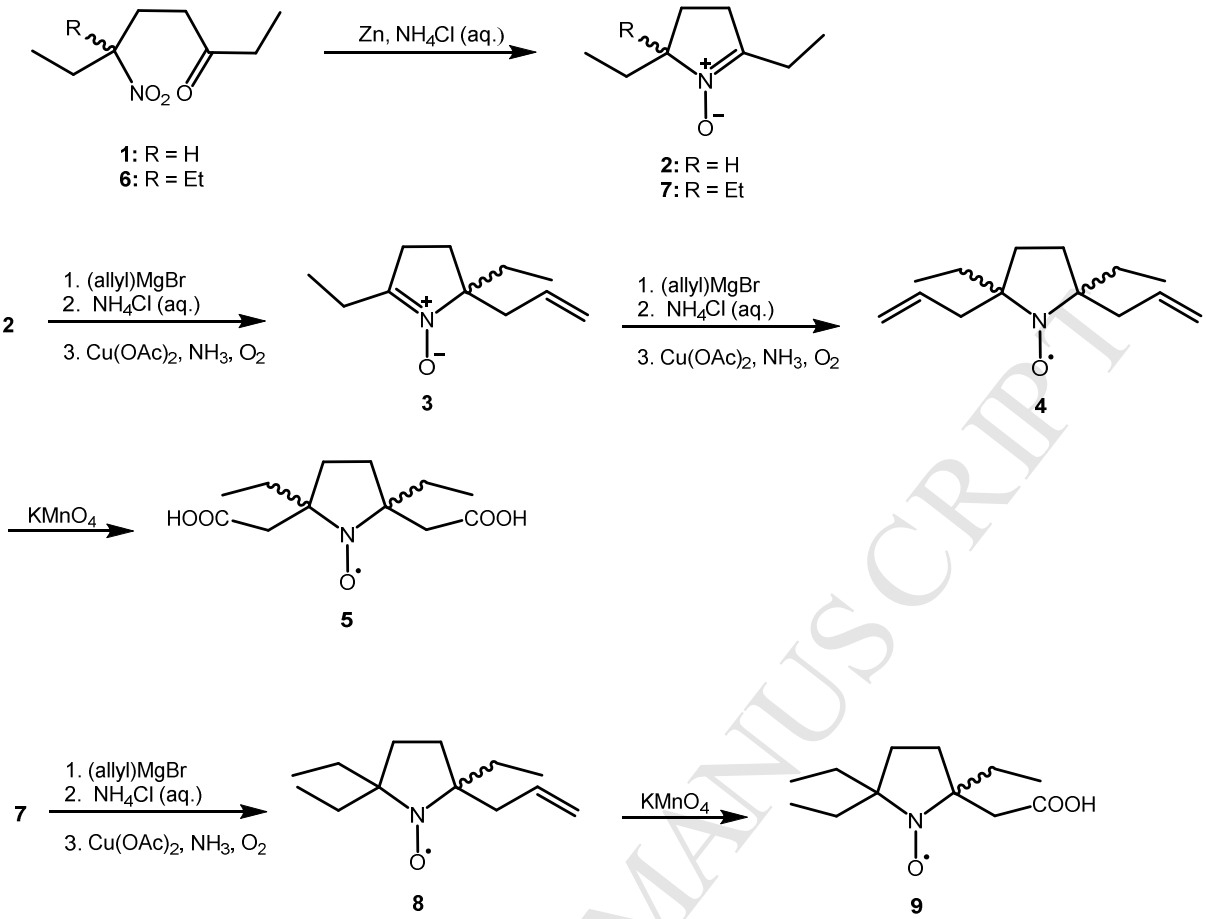

Scheme 2 Synthetic route to the pyrrolidine nitroxide radicals **5** and **9**.

*Structural descriptions of **cis-5** and **9***

Compounds ***cis*-5** and **9** were structurally characterized by single-crystal X-ray analysis. The molecular structures are depicted in Figure 1 and selected bond lengths and angles are listed in Table 2. The molecular geometry parameters of the pyrrolidine *N*-oxyl moieties are within expected ranges [22-27]. The conformation of the five-membered rings in ***cis*-5** and **9** is best described as envelope with respectively C3 and C4 on the flap. The conformations of the peripheral substituents about the $C_{pyrrolidine}–C_{methylene}$ bonds in ***cis*-5** are antiperiplanar with respect to the pyrrolidine nitrogen atom, except for the ethyl group attached to C2, which adopts a synclinal conformation. In **9**, the two *trans*-related 2- and 5-ethyl groups show synclinal conformations about the $C_{pyrrolidine}–C_{methylene}$ bonds with respect to the nitrogen atom, whereas the carboxymethyl group and the remaining 5-ethyl group exhibit antiperiplanar conformations.

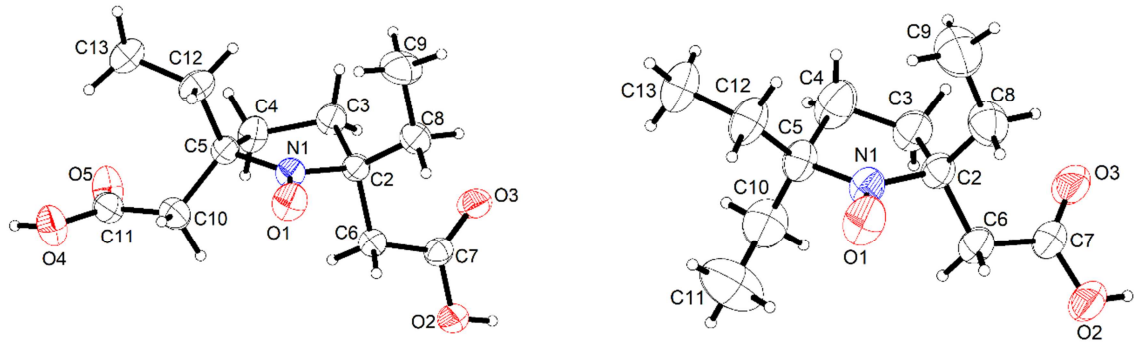

***cis*-5** **9**

Figure 1 Molecular structures of ***cis*-5** and **9**, respectively showing the (2*R*,5*S*) form and the (2*R*) form in the centrosymmetric crystal structures. Displacement ellipsoids are drawn at the 50 % probabillity level. Hydrogen atoms are represented by small spheres of arbitrary radii.

Table 2 Selected bond lengths (Å) and angles (°) for ***cis*-5** and **9**.

	***cis*-5**	**9**
O1–N1	1.2735(14)	1.273(3)
N1–C2	1.4854(15)	1.475(3)
N1–C5	1.4844(16)	1.485(3)
C2–C3	1.5297(18)	1.528(4)
C3–C4	1.5281(18)	1.491(4)
C4–C5	1.5298(18)	1.549(4)
O1–N1–C2	121.86(10)	121.7(2)
O1–N1–C5	122.33(10)	123.1(2)
C2–N1–C5	115.41(10)	115.2(2)
N1–C2–C3	100.80(9)	102.0(2)
C4–C3–C2	105.22(10)	107.1(2)
C3–C4–C5	106.24(11)	106.2(3)
N1–C5–C4	101.32(9)	99.9(2)

In the crystal structures of ***cis*-5** and **9**, the molecules are joined through hydrogen bonds of the O–H···O type between carboxy goups with centrosymmetric $R_2^2(8)$ motifs [28]. This results in polymeric zigzag chains, extending in the [10-1] direction, in ***cis*-5**, and in dimers in **9** (Figure 2). The hydrogen bond geometry parameters (Table 3) indicate strong O–H···O hydrogen bonds [29]. The hydrogen bonding patters observed in ***cis*-5** and **9** are consistent with Etter's third rule for hydrogen bonding, which states that the best hydrogen bond donors and the best hydrogen bond acceptors form hydrogen bonds to one another [30]. The nitroxide oxygen atom can be considered a weaker hydrogen bond acceptor than the hydrogen bond acceptor site of the carboxy group and, thus, the nitroxide groups in ***cis*-5** and **9** only exhibit C–H···O contacts that are shorter than the sum of the corresponding van der Waals radii [31], but do not form classical hydrogen bonds.

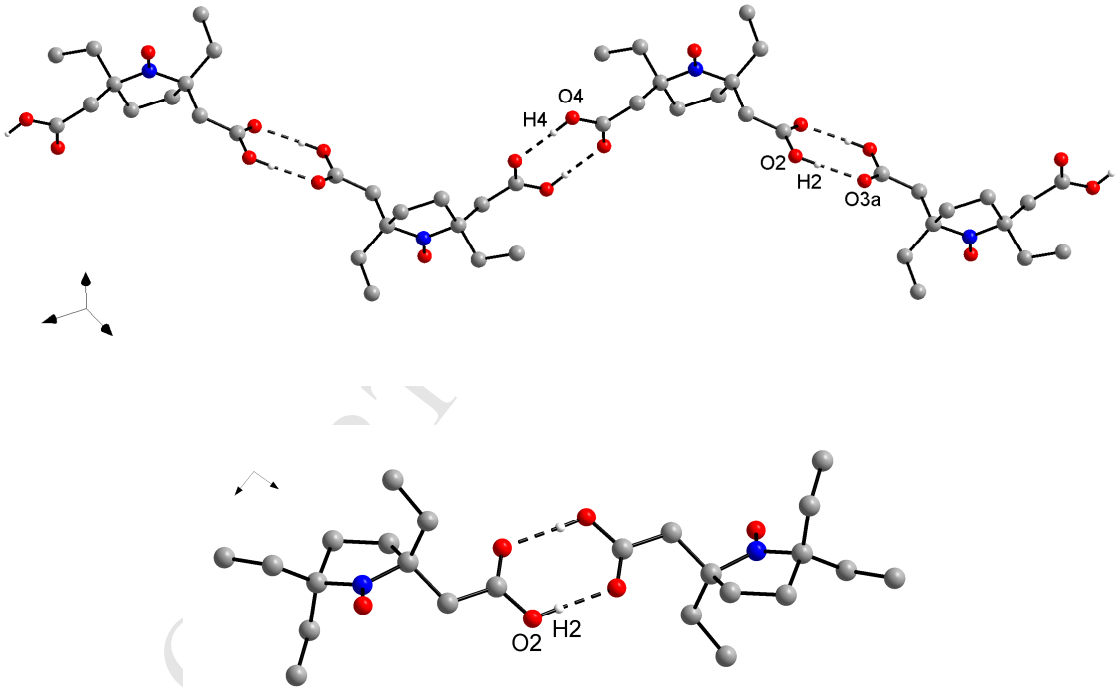

Figure 2 Hydrogen-bonded chains in ***cis*-5** (top) and hydrogen-bonded dimers in **9** (bottom). Hydrogen bonds are represented by dashed lines. Carbon-bound hydrogen atoms are omitted for clarity. Symmetry codes: (a) –x+1, –y, –z; (b) –x, –y, –z+1.

Table 3 Hydrogen bond geometry (Å, °) for ***cis*-5** and **9**.[a]

D*–H···*A	***d*(*D*–H)**	***d*(H···*A*)**	***d*(*D*···*A*)**	**<(*DHA*)**
		***cis*-5**		
O2–H2···O3a	0.858(14)	1.789(15)	2.6450(14)	175.0(18)
O4–H4···O5b	0.878(15)	1.748(15)	2.6248(15)	176.3(19)
		9		
O2–H2···O3a	0.83	1.83	2.657(3)	177.9

[a] Symmetry codes: (a) –x+1, –y, –z; (b) –x, –y, –z+1.

EPR spectroscopy

The EPR spectra of ***cis*-5**, ***trans*-5** and **9, 3-CP** were measured in buffer solutions at different pH levels. Figure 3 shows the EPR spectrum of each radical at pH 7.4. The intensities of the three lines are almost equal, which means that the anisotropies of hyperfine coupling and *g* factor are almost averaged [1]. The spectra are therefore close to the isotropic limit. The hyperfine coupling constants *a*(N) (Table 4) are similar for ***cis*-** and ***trans*-5** and increase in the following order: ***cis*-/*trans*-5** < **9** < **3-CP**. The nitrogen hyperfine signals are accompanied by ^{13}C satellites. The spectra of **3-CP** show two different groups of ^{13}C satellites; the spectra of ***cis*-/*trans*-5** and **9** only one. The lineshape of the spectra is mainly Gaussian. The EPR signals of ***cis*-5**, ***trans*-5** and **9** are 50 to 70 µT broader than the signal of **3-CP**.

Nitroxide radicals with a hydrogen acceptor or donor site are sensitive to the pH level in their environment. Table 5 shows the pH sensitivity $\Delta a(\mathrm{N})_{max}$ and pKa values of the nitroxide radicals derived from titration curves (see Supporting Information). A pH dependence of the hyperfine coupling constant *a*(N) is observed in acidic medium between pH 2.5 and 6.5. Within physiological pH range, the influence of pH on *a*(N) is negligible. The exact pH range depends on the pKa of the radical. pH sensitivity and pKa values vary notably depending on the molecular structure of the nitroxide radical. The carbon hyperfine coupling is not influenced by the pH.

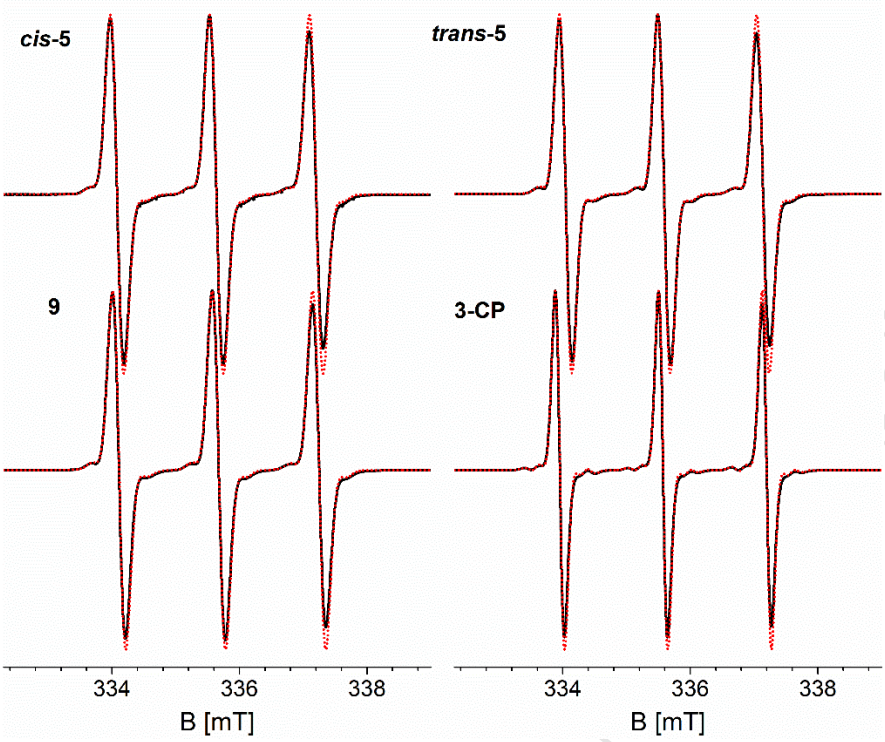

Figure 3 EPR spectra (black solid line: experiment, red dotted line: simulation) of 1 mM solutions of ***cis*-5**, ***trans*-5**, **9** and **3-CP** in 1 mM phosphate buffer (pH 7.4).

Table 4 Hyperfine coupling constants a and peak-to-peak linewidths (ΔB_{pp}) of **3-CP**, ***cis*-5**, ***trans*-5** and **9** at different pH levels. The number of carbon atoms is given in parenthesis.

	pH	***a*(N) [mT]**	***a*(C1)/*a*(C2) [mT]**	**ΔB_{pp} (Gaussian/ Lorentzian) [mT]**
***cis*-5**	4.5	1.527	0.653 (6)	0.185/0.015
	7.4	1.565	0.653 (6)	0.210/0.010
	8.8	1.559	0.653 (6)	0.210/0.010
***trans*-5**	4.5	1.529	0.653 (6)	0.180/0.015
	7.4	1.552	0.653 (6)	0.190/0.015
	8.8	1.552	0.653 (6)	0.190/0.015
9	4.5	1.556	0.669 (6)	0.190/0.015
	7.4	1.572	0.669 (6)	0.200/0.015
	8.8	1.572	0.669 (6)	0.195/0.015
3-CP	4.5	1.615	0.962 (5)/0.530 (2)	0.135/0.012
	7.4	1.625	0.962 (5)/0.530 (2)	0.140/0.012
	8.8	1.624	0.962 (5)/0.530 (2)	0.140/0.012

Table 5 pH sensitivity $\Delta a(N)_{max}$ and pKa values.

	$\Delta a(N)_{max}$ [μT]	pKa
***cis*-5**	41	4.75
***trans*-5**	30	4.34
9	16	4.32
3-CP	20	3.69

The nitrogen hyperfine coupling constant a(N) depends on extrinsic and intrinsic factors like the polarity and the hydrogen bonding capability of the solvent and the overall constitution of the radical. In the resonance structures [$R_2N–O^{\bullet} \leftrightarrow R_2N^{+}–O^{\bullet-}$], polar solvents such as water stabilize the ionic structure of the nitroxide group, leading to increased spin density on the nitrogen atom and larger hyperfine coupling constant [1, 32]. Since the nitroxide radicals studied showed different a(N) values (Table 4) in the same solvent, these differences were attributed to the different molecular structures. The hyperfine coupling constant a(N) generally increases with an increasing out-of-plane angle of the N–O$^{\bullet}$ moiety [33]. For five-membered rings, this angle is usually small [34]. In the crystal structures, the angle between the N1–O1 bond and the C2–N1–C5 plane is 6.01(12)° for ***cis*-5**, 0.8(3)° for **9** and 3.24(14)° for (*R*)-**3-CP** [23]. Since a(N) increases from **5** to **3-CP**, this observation may be ascribed to factors other than the out-of-plane angle of the N–O$^{\bullet}$ moiety – bearing in mind that the out-of-plane angles were determined for the molecular structures in the solid-state. The a(N) values also depends on the torsional oscillation of the nitroxide, which is influenced by the substituents in the α positions. It has been shown that substitution in the α-position hinders the torsional oscillation and thereby lowers a(N) [33]. Therefore, it is reasonable to assume that the values for a(N) decreasing from **3-CP** to ***cis*-**/***trans*-**5** result from decreased conformational flexibility of the pyrrolidine ring.

The spectral linewidth of nitroxide radicals depends on different factors: unresolved proton hyperfine couplings, anisotropic interactions and interactions with other paramagnetic species [32, 35]. Exchange broadening by molecular collisions between nitroxides is negligible under the experimental conditions. Exchange broadening due to interaction with oxygen occurs, but does not explain the smaller linewidth of **3-CP** compared with nitroxide radicals bearing ethyl/carboxymethyl substituents in 2- and 5-positions. The main contributions are therefore unresolved proton hyperfine couplings and anisotropic hyperfine interactions. Hyperconjugation and long-range coupling of ethyl- and carboxymethyl-protons

might cause additional line-broadening in ***cis***-/***trans*-5** and **9** [35]. The smaller linewidth of **3-CP** accompanies the larger nitrogen hyperfine coupling constant *a*(N). Torsional oscillations and a high flexibility of the ring structure increases *a*(N) and decreases *a*(H), owing to dynamic averaging of the proton coupling constants of different conformations [35, 36].

The pH-dependency of the hyperfine coupling constant *a*(N) in the nitroxide radicals is due to the presence of the carboxy groups. The pH range in which sensitivity is observed depends on the pKa value of nitroxide radical and the medium. The pKa values can be estimated from the titration curves (see Supporting Information) at the pH of the half-equivalence point: $a(N) + a(N)^{(2)-}/2$ [32]. The pKa value estimated for **3-CP** is comparable with experimental values from other literature (pKa = 3.89 [32]; 3.40 [37]). pKa_1 and pKa_2 of the **5** isomers cannot be distinguished on the basis of the experimental data. The average pKa values obtained for ***cis*-/*trans*-5** and the pKa found for **9** are within the expected range for carboxylic acids (Table 5). The higher pH sensitivity of ***cis*-/*trans*-5** as compared with **9** and **3-CP** is most likely a result of an increased electrostatic influence of the second carboxy group in the former compounds. The observed differences between ***cis*-** and ***trans*-5** can be ascribed to a different extent of stabilization of the ionic form of the nitroxides.

Reductive stability

The reductive stability of ***cis*/*trans*-5** and **9** was compared with the two commercial nitroxide radicals **3-CP** and **4-CT** in an ascorbic acid reduction assay. The rates of reduction were studied assuming *pseudo* first-order conditions using a 10-fold excess of ascorbic acid in phosphate buffer pH 7.4 (50 mM, 2 mM ETDA). The decay curves are shown in Figure 4. Second order rate constants for the initial reduction rates were obtained from the decay of the low-field peak height by analysis of the linear part of the decay curves (Table 6). The results indicate an increased stability of the pyrrolidine nitroxides as compared with the piperidine nitroxide **4-CT**. For the pyrrolidine nitroxides, the stability increases in the order **3-CP** < ***cis*-5** ≈ ***trans*-5** < **9**.

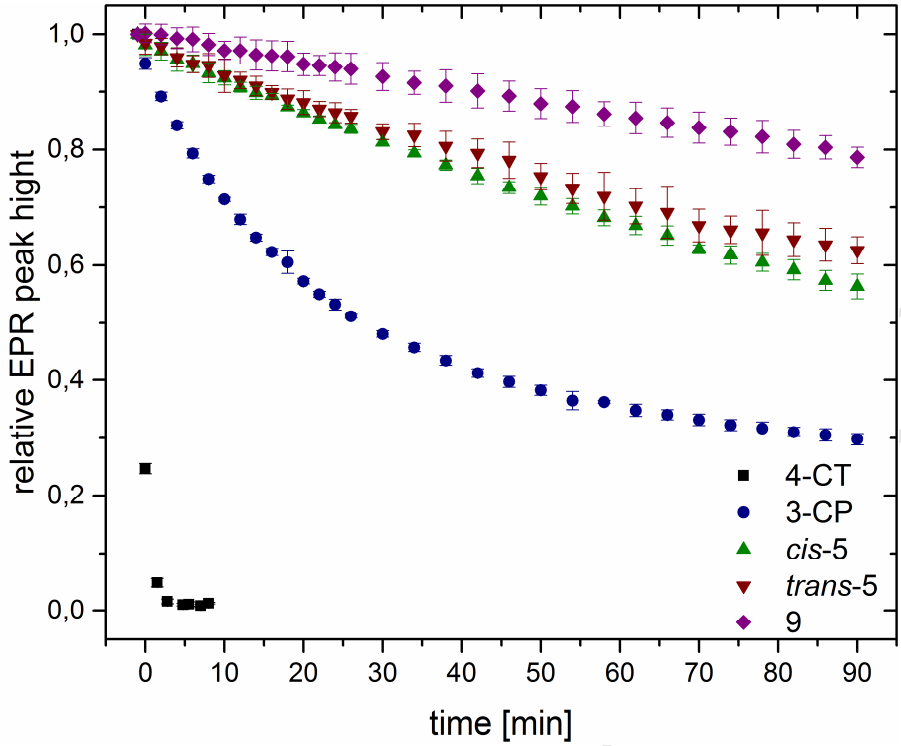

Figure 4 Reduction profiles of the tested nitroxides. Nitroxide 0.5 mM with tenfold excess of ascorbic acid in phosphate buffer 50 mM pH 7.4 at 298 K. Mean ± standard deviation of three runs.

Table 6 Second-order rate constants *k* for initial rates of reduction.

	avg *k* [$M^{-1}s^{-1}$]	time [s]	radical left[a] [%]
***cis*-5**	0.02074 ± 0.002	5400	56.7 ± 2.1
***trans*-5**	0.01737 ± 0.002	5400	62.7 ± 2.3
9	0.0086 ± 0.0005	5400	78.7 ± 1.7
3-CP	0.0946 ± 0.001	840	29.7 ± 0.9
4-CT	3.6253 ± 0.140	150	0.0 ± 0.0

[a] residual radical after 90 min

The reductive stability of cyclic nitroxides depends mainly on the ring size. It is well-known that the stability dramatically increases from piperidine to pyrrolidine derivatives. In contrast to five-membered ring nitroxides, piperidine derivatives can undergo conformational changes which lead to better accessibility of the nitroxide moiety [38]. This explains the difference between **4-CT** and the pyrrolidine nitroxides.

The stability is further influenced by steric, electrostatic and field or inductive effects of the ring substituents [38]. Bulky alkyl groups adjacent to nitroxyl decrease the reduction rate by steric shielding [39, 40]. Ionizable substituents lead to a reduced (*e. g.* $-NH_3^+$) or increased (*e. g.* $-COO^-$) reductive stability due to electrostatic attraction or repulsion of the ascorbic acid anion [38, 41]. These observations, especially the steric shielding, explains the increased stability of compounds ***cis*/*trans*-5** and **9** compared with **3-CP**. Inductive effects of the substituents have to be considered, too. Literature reports indicate that electron-withdrawing groups increase the accessibility of the nitroxide moiety for reductive agents, whereas electron-donating groups have the opposite effect [6, 8, 38]. Attempts have been made to correlate the stability of nitroxides with field or inductive constants of the substituents like the Swain/Lupton F-parameter [8]. The F-values [42] for the substituents of the nitroxides studied in this work (Table 7) indeed correlate well with the decreased reductive stability of ***cis*/*trans*-5** compared with **9**. Substituents with positive F-values exhibit an electron-withdrawing effect leading to reduced stability of the nitroxide group. In ***cis*/*trans*-5**, the influence of the electron-withdrawing carboxymethyl group is doubled compared with **9**. The reductive stability is thus decreased. The reduction rate of **9** is about eleven times lower than the reduction rate of **3-CP**. The reduction rate of one the of the most stable nitroxides reported, the tetraethyl derivative of **3-CP**, is, however, about 63 times lower than the reduction rate of **3-CP** [7]. This suggests that introduction of carboxymethyl groups in the α-positions of the nitroxide group is not favorable for inducing additional reductive stability**.**

Table 7 Swain/Lupton F-parameters [42].

***cis*/*trans*-5**	$2 \times 0.19 + 2 \times 0.00$
9	$0.19 + 3 \times 0.00$
3-CP	4×0.01
4-CT	4×0.01

Conclusions

The nitroxide radicals ***cis*/*trans*-5** and **9** exhibit higher reductive stability against ascorbic acid than the common nitroxide radicals **3-CP** and **4-CT**, which is ascribed to steric and electrostatic shielding imparted by the tethered ethyl and carboxymethyl groups in the α-positions. Compound **9**, bearing one carboxymethyl group exhibits a higher reductive stability than ***cis*/*trans*-5**, bearing two carboxymethyl groups. This can be explained by the destabilizing electron-withdrawing effect of these functional groups, which compensates the stabilization through electrostatic shielding. While the reductive stability of the tetraethyl derivative **3-CP** is still higher, **5** and **9** are more versatile spin labels because of the carboxy groups which impart hydrophilicity - important for biological fluids - and pronounced pH sensitivity of the EPR signal, and they allow labelling of (bio)polymers.

Acknowledgements

We would like to thank Professor Dariush Hinderberger (Institut für Chemie, Martin-Luther-Universität Halle-Wittenberg) for providing access to the EPR spectrometer. RWS is grateful to Dr Richard Goddard for helpful discussions.

References

[1] E. Bordignon (2017). EPR spectroscopy of nitroxide spin probes. In eMagRes, (Eds. R. K. Harris and R.L. Wasylishen). doi: 10.1002/9780470034590.emrstm1513
[2] J.P. Klare, H.-J. Steinhoff, Spin labeling EPR, Photosynthesis Research 102 (2009) 377-390.
[3] D. Bardelang, M. Hardy, O. Ouari, P. Tordo (2012). Spin labels and spin probes. In Encyclopedia of Radicals in Chemistry, Biology and Materials (Eds. C. Chatgilialoglu and A. Studer). doi: 10.1002/9781119953678.rad081
[4] M.M. Haugland, J.E. Lovett, E.A. Anderson, Advances in the synthesis of nitroxide radicals for use in biomolecule spin labelling, Chemical Society Reviews 47 (2018) 668-680.
[5] M.M. Haugland, E.A. Anderson, J.E. Lovett (2017). Tuning the properties of nitroxide spin labels for use in electron paramagnetic resonance spectroscopy through chemical modification of the nitroxide framework, Electron Paramagnetic Resonance: Volume 25, The Royal Society of Chemistry, pp. 1-34. doi: 10.1039/9781782629436-00001
[6] I.A. Kirilyuk, A.A. Bobko, S.V. Semenov, D.A. Komarov, I.G. Irtegova, I.A. Grigor'ev, E. Bagryanskaya, Effect of sterical shielding on the redox properties of imidazoline and imidazolidine nitroxides, The Journal of Organic Chemistry 80 (2015) 9118-9125.

[7] J.T. Paletta, M. Pink, B. Foley, S. Rajca, A. Rajca, Synthesis and reduction kinetics of sterically shielded pyrrolidine nitroxides, Organic Letters 14 (2012) 5322-5325.
[8] S. Huang, H. Zhang, J.T. Paletta, S. Rajca, A. Rajca, Reduction kinetics and electrochemistry of tetracarboxylate nitroxides, Free Radical Research 52(3) (2018) 327-334.
[9] J.E. McMurry, J. Melton, Conversion of nitro to carbonyl by ozonolysis of nitronates - 2,5-heptandione, Organic Syntheses 56 (1977) 36.
[10] R. Ballini, P. Marziali, A. Mozzicafreddo, Amberlyst A-27, an efficient heterogeneous catalyst for the Michael reaction of nitroalkanes with beta-substituted alkene acceptors, The Journal of Organic Chemistry 61 (1996) 3209-3211.
[11] K.E. Gilbert, W.T. Borden, Peracid oxidation of aliphatic amines - general synthesis of nitroalkanes, The Journal of Organic Chemistry 44 (1979) 659-661.
[12] S. Miele, P. Nesvadba, A. Studer, 1-tert-Butyl-3,3,5,5-tetraalkyl-2-piperazinon-4-oxyls: Highly Efficient Nitroxides for Controlled Radical Polymerization, Macromolecules 42 (2009) 2419-2427.
[13] G.M. Sheldrick, SHELXT - integrated space-group and crystal-structure determination, Acta Crystallographica A71 (2015) 3-8.
[14] G.M. Sheldrick, Crystal structure refinement with SHELXL, Acta Crystallographica C71 (2015) 3-8.
[15] O.V. Dolomanov, L.J. Bourhis, R.J. Gildea, J.A.K. Howard, H. Puschmann, OLEX2: a complete structure solution, refinement and analysis program, Journal of Applied Crystallographica 42 (2009) 339-341.
[16] K. Brandenburg, DIAMOND, Crystal Impact GbR, Bonn, Germany, 2016.
[17] J.F. Corbett, Pseudo first-order kinetics, Journal of Chemical Education 49 (1972) 663.
[18] K. Hideg, L. Lex, A versatile new method for the synthesis of various pyrrolidin-1-oxyl fatty acids, Journal of the Chemical Society, Chemical Communications (1984) 1263-1265.
[19] K. Hideg, L. Lex, Synthesis of various new nitroxide free-radical fatty-acids, Journal of the Chemical Society, Perkin Transactions 1 (1986) 1431-1438.
[20] W. Rundel (1968). Methoden zur Herstellung und Umwandlung von Nitronen. In Houben-Weyl: Methoden der Organischen Chemie (Ed. E.Müller), Georg Thieme Verlag, Stuttgart, pp. 309-448.
[21] W.D. Morris, J.M. Mayer, Separating proton and electron transfer effects in three-component concerted proton-coupled electron transfer reactions, Journal of the American Chemical Society 139 (2017) 10312-10319.
[22] J.F.W. Keana, K. Hideg, G.B. Birrell, O.H. Hankovszky, G. Ferguson, M. Parvez, New mono- and difunctionalized 2,2,5,5-tetramethylpyrrolidine and Δ^3-pyrroline-1-oxyl nitroxide spin labels, Canadian Journal of Chemistry 60 (1982) 1439-1447.
[23] J.B. Wetherington, S.S. Ament, J.W. Moncrief, Structure and absolute configuration of the spin-label *R*-(+)-3-carboxy-2,2,5,5-tetramethyl-1-pyrrolidinyloxy, Acta Crystallographica B30 (1974) 568-573.
[24] Y. Uchida, R. Tamura, N. Ikuma, M.A. Kazuyoshi, T.A. Hiroki, S. Shimono, J. Yamauchi, Antiferromagnetic interactions arising from a close contact between nitroxyl oxygen and β-methyl carbon atoms carrying an α-spin in the solid state, Mendeleev Communications 16 (2006) 69-71.
[25] B. Chion, J. Lajzerowicz, Structures cristallographiques de formes racémique et optiquement active du tétraméthyl-2,2,5,5 pyrrolidine-3 carboxamide oxyle-1, Acta Crystallographica 31 (1975) 1430-1435.
[26] I.A. Kirilyuk, Y.F. Polienko, O.A. Krumkacheva, R.K. Strizhakov, Y.V. Gatilov, I.A. Grigor'ev, E.G. Bagryanskaya, Synthesis of 2,5-bis(spirocyclohexane)-substituted nitroxides of pyrroline and pyrrolidine series, including thiol-specific spin label: an analogue of MTSSL with long relaxation time, The Journal of Organic Chemistry 77 (2012) 8016-8027.
[27] B. Chion, J. Lajzerowicz, A. Collet, J. Jacques, Etude des mélanges d'antipode optiques. XI. Un exemple de solution solide entre énantiomères: le nitroxyde de la tétraméthyl-2,2,5,5 hydroxy-3 pyrrolidine. Etude cristallographique, Acta Crystallographica B32 (1976) 339-344.
[28] J. Bernstein, R.E. Davis, L. Shimoni, N.L. Chang, Patterns in hydrogen bonding - functionality and graph set analysis in crystals, Angewandte Chemie International Edition 34 (1995) 1555-1573.

[29] R. Thakuria, B. Sarma, A. Nangia (2017). Hydrogen bonding in molecular crystals. In, Comprehensive Supramolecular Chemistry II (Ed. J.L. Atwood), Elsevier, Oxford, pp. 25-48.
[30] M.C. Etter, Encoding and decoding hydrogen-bond patterns of organic-compounds, Accounts of Chemical Research 23 (1990) 120-126.
[31] A. Bondi, Van der Waals volumes and radii, The Journal of Physical Chemistry 68(3) (1964) 441-451.
[32] G.A.A. Saracino, A. Tedeschi, G. D'Errico, R. Improta, L. Franco, M. Ruzzi, C. Corvaia, V. Barone, Solvent polarity and pH effects on the magnetic properties of ionizable nitroxide radicals: a combined computational and experimental study of 2,2,5,5-tetramethyl-3-carboxypyrrolidine and 2,2,6,6-tetramethyl-4-carboxypiperidine nitroxides, The Journal of Physical Chemistry A 106(44) (2002) 10700-10706.
[33] A. Rockenbauer, M. Györ, H.O. Hankovszky, K. Hideg, E.S.R. of the conformation of 5- and 6-membered cyclic nitroxide (aminoxyl) radicals, in: M.C.R. Symons (Ed.), Electron Spin Resonance: Volume 11A, The Royal Society of Chemistry 1988, pp. 145-182.
[34] L.J. Berliner, Spin Labeling: Theory and Applications, Elsevier Science 1976.
[35] J.A. Weil, J.R. Bolton, Electron Paramagnetic Resonance: Elementary Theory and Practical Applications, Wiley 2007.
[36] S.R. Burks, M.A. Makowsky, Z.A. Yaffe, C. Hoggle, P. Tsai, S. Muralidharan, M.K. Bowman, J.P.Y. Kao, G.M. Rosen, The effect of structure on nitroxide EPR spectral linewidth, The Journal of Organic Chemistry 75 (2010) 4737-4741.
[37] R.N. Schwartz, M. Peric, S.A. Smith, B.L. Bales, Simple test of the effect of an electric field on the N-14-hyperfine coupling constant in nitroxide spin probes, J. Phys. Chem. B 101 (1997) 8735-8739.
[38] S. Morris, G. Sosnovsky, B. Hui, C.O. Huber, N.U.M. Rao, H.M. Swartz, Chemical and electrochemical reduction rates of cyclic nitroxides (nitroxyls), Journal of Pharmaceutical Sciences 80 (1991) 149-152.
[39] A.P. Jagtap, I. Krstic, N.C. Kunjir, R. Hänsel, T.F. Prisner, S.T. Sigurdsson, Sterically shielded spin labels for in-cell EPR spectroscopy: Analysis of stability in reducing environment, Free Radical Research 49 (2015) 78-85.
[40] S.A. Dobrynin, Y.I. Glazachev, Y.V. Gatilov, E.I. Chernyak, G.E. Salnikov, I.A. Kirilyuk, Synthesis of 3,4-Bis(hydroxymethyl)-2,2,5,5-tetraethylpyrrolidin-1-oxyl via 1,3-dipolar cycloaddition of azomethine ylide to activated alkene, The Journal of Organic Chemistry 83 (2018) 5392-5397.
[41] J.F.W. Keana, S. Pou, G.M. Rosen, Nitroxides as potential contrast enhancing agents for MRI application: Influence of structure on the rate of reduction by rat hepatocytes, whole liver homogenate, subcellular fractions, and ascorbate, Magnetic Resonance in Medicine 5 (1987) 525-536.
[42] C. Hansch, A. Leo, R.W. Taft, A survey of Hammett substituent constants and resonance and field parameters, Chemical Reviews 91 (1991) 165-195.

- Two new pyrrolidine nitroxide radicals were synthesized and structurally characterized.
- Carboxymethyl and ethyl groups in the α-positions of the nitroxide group improve the stability of the radicals.
- The new radicals exhibit higher reductive stability than 3-carboxy-PROXYL and 4-carboxy-TEMPO.